Technical University of Denmark

DTU

CO2 Capture with Liquid-Liquid Phase Change Solvents: A Thermodynamic Study

Arshad, Muhammad Waseem; Fosbøl, Philip Loldrup; von Solms, Nicolas; Thomsen, Kaj

DTU Library
Technical Information Center of Denmark

13th International Conference on Greenhouse Gas Control Technologies, GHGT-13, 14-18 November 2016, Lausanne, Switzerland

CO$_2$ Capture with Liquid-Liquid Phase Change Solvents: A Thermodynamic Study

Muhammad Waseem Arshad, Philip Loldrup Fosbøl, Nicolas von Solms, Kaj Thomsen*

Technical University of Denmark, Department of Chemical and Biochemical Engineering, Center for Energy Resources Engineering (CERE), Søltofts Plads Building 229, DK-2800 Kongens Lyngby, Denmark

Abstract

Extended UNIQUAC thermodynamic framework was implemented in this work to model the aqueous blend of *N,N*-Diethylethanolamine (DEEA) and *N*-Methyl-1,3-diaminopropane (MAPA) for CO$_2$ capture. The model parameters were estimated first for the two ternary systems, H$_2$O-DEEA-CO$_2$ and H$_2$O-MAPA-CO$_2$, followed by the quaternary H$_2$O-DEEA-MAPA-CO$_2$ system which gives liquid-liquid phase split when reacted with carbon dioxide. A total of 94 model parameters and 6 thermodynamic properties were fitted to approximately 1500 equilibrium and thermal experimental data consisting of pure amine vapor pressure (P^{vap}), vapor-liquid equilibrium (VLE), solid-liquid equilibrium (SLE), liquid-liquid equilibrium (LLE), excess enthalpy (H^E), and heat of absorption (ΔH_{abs}) of CO$_2$ in aqueous amine solutions. The model developed in this work can accurately represent the equilibrium and thermal data for the studied systems with a single unique set of parameters.

Keywords: Thermodynamic modeling; Extended UNIQUAC; Phase change solvents; DEEA; MAPA; Liquid-liquid equilibrium; CO$_2$ capture

1. Introduction

Power generation based on fossil fuel is one of the major sources of CO$_2$ emissions worldwide and carbon capture and storage (CCS) has been identified as a potential solution to reduce the CO$_2$ emissions [1]. Amongst the available

---

* Corresponding author. Tel.: +45 4525 2860; fax: +45 4588 2258.
  E-mail address: kth@kt.dtu.dk

CCS technologies, post-combustion CO_2 capture (PCC) has been demonstrated commercially for a large scale capture of CO_2 [2]. Boundary Dam power station in Canada by Saskpower and TCM (Technology Center Mongstad) in Norway are two major examples of large scale PCC facilities. However, one of the major challenges with this technology is the high energy demand of the process [3].

Solvents used in the PCC technology play a major role in determining the energy demand of the process. A large amount of amine based solvent systems has been reported in the open literature. An ideal solvent system should exhibit low solvent regeneration energy in addition to a high CO_2 loading capacity and reasonably fast reaction kinetics [3]. With these characteristics in focus, a liquid-liquid phase change solvent system consisting of DEEA (*N,N*-Diethylethanolamine) and MAPA (*N*-Methyl-1,3-diaminopropane) has been studied in this work. An aqueous blend of 5M DEEA and 2M MAPA exhibits two liquid phases upon CO_2 absorption with a lower phase rich in CO_2 and an upper phase lean in CO_2. The upper phase is sent to absorber without regeneration and has a large driving force for CO_2 absorption, and the lower rich phase is regenerated in the desorber. A low liquid circulation rate to the desorber can lead to low energy demand of the regeneration process. This liquid-liquid phase change solvent system has been reported in our previous work [4-10].

Process simulation requires accurate thermodynamic models to design the unit operations in the capture process. This work presents thermodynamic modeling of aqueous blend of DEEA and MAPA with characteristics of liquid-liquid phase change. Extended UNIQUAC thermodynamic framework has been used in this work. Model parameters were estimated for H_2O-DEEA-CO_2, H_2O-MAPA-CO_2, and H_2O-DEEA-MAPA-CO_2 (phase change system) systems by using a variety of experimental equilibrium and thermal data e.g., pure amine vapor pressure (P_{vap}), vapor-liquid equilibrium (VLE), solid-liquid equilibrium (SLE), liquid-liquid equilibrium (LLE), excess enthalpy (H^E), and heat of absorption (ΔH_{abs}) of CO_2 in aqueous amine solutions. Ninety four model parameters and six thermodynamic properties were fitted to approximately 1500 experimental data. The model developed in this work represents the equilibrium and thermal data for all the studied systems with a single unique set of parameters.

2. The Model

The Gamma-Phi ($\gamma - \phi$) approach is used in this work for the phase equilibrium calculations. This means that the Extended UNIQUAC model is used to calculate the aqueous-phase activity coefficient (γ) and Soave-Redlich-Kwong (SRK) cubic equation of state (EoS) is used to determine the vapor-phase fugacity coefficient (ϕ).

Extended UNIQUAC model is an activity coefficient model for electrolyte systems [11,12]. It consists of a short-range contribution from the original UNIQUAC model combined with the Debye-Hückel long-range term which takes into account the electrostatic interactions of the ionic species present.
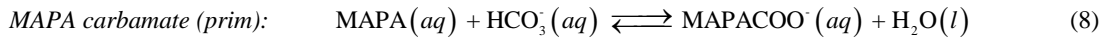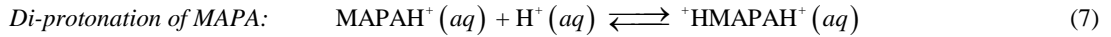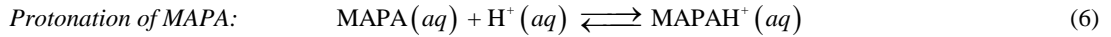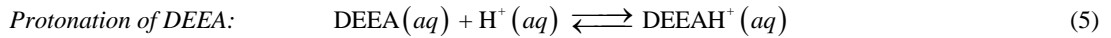
$$G^E_{\text{Extended UNIQUAC}} = G^E_{\text{Combinatorial}} + G^E_{\text{Residual}} + G^E_{\text{Debye-Hückel}} \tag{1}$$

The first two terms, the combinatorial (or entropic) and the residual (or enthalpic) terms, are identical to the terms used in the UNIQUAC model. The combinatorial term requires two adjustable parameters per species (volume, r, and surface area, q, parameters) and the residual term requires two adjustable parameters (u^0_{ij} and u^T_{ij}) per pair of binary species to calculate the interaction energy parameter u_{ij} from $u_{ij} = u^0_{ij} + u^T_{ij}(T - 298.15)$. The third term in the Extended UNIQUAC model is derived from the extended Debye-Hückel law. This term has no adjustable parameter. It only represents the electrostatic interactions of the ionic species. Similarly, the SRK equation has no interaction parameters to be fitted for the gas phase. The SRK EoS is applied with classical mixing rules (quadratic mixing rule for the a parameter and linear mixing rule for the b parameter).

3. Equilibrium and Thermal Calculations

3.1. Speciation Equilibria

Several reactions take place when CO_2 in dissolved in aqueous amine solutions. These reactions depend on the type of amine. The following speciation equilibria were considered for the thermodynamic modeling.

Dissociation of water:	$H_2O(l) \rightleftharpoons H^+(aq) + OH^-(aq)$	(2)
Hydrolysis of CO₂:	$CO_2(aq) + H_2O(l) \rightleftharpoons HCO_3^-(aq) + H^+(aq)$	(3)
Dissociation of bicarbonate:	$HCO_3^-(aq) \rightleftharpoons CO_3^{2-}(aq) + H^+(aq)$	(4)
Protonation of DEEA:	$DEEA(aq) + H^+(aq) \rightleftharpoons DEEAH^+(aq)$	(5)
Protonation of MAPA:	$MAPA(aq) + H^+(aq) \rightleftharpoons MAPAH^+(aq)$	(6)
Di-protonation of MAPA:	$MAPAH^+(aq) + H^+(aq) \rightleftharpoons {}^+HMAPAH^+(aq)$	(7)
MAPA carbamate (prim):	$MAPA(aq) + HCO_3^-(aq) \rightleftharpoons MAPACOO^-(aq) + H_2O(l)$	(8)
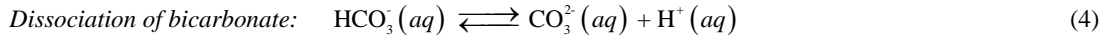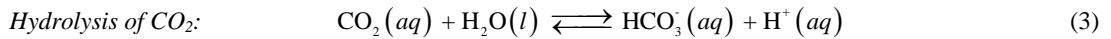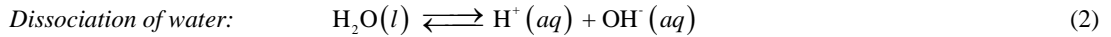
For all the speciation equilibria given in equations 2-8, the condition for equilibrium is that the summation of chemical potential of the reactants is equal to the summation of chemical potential of the products.

$$\sum_i \mu_{i,\,Reactants} = \sum_i \mu_{i,\,Products} \tag{9}$$

For speciation calculations, equation 9 is applied to hydrolysis of CO₂ (equation 3) by considering the symmetrical convention for water and unsymmetrical convention for remaining species to get following expression.

$$-\frac{\left(\mu^*_{HCO_3^-(aq)} + \mu^*_{H^+(aq)}\right) - \left(\mu^*_{CO_2(aq)} + \mu^0_{H_2O(l)}\right)}{RT} = \ln\left(\frac{a^*_{HCO_3^-(aq)} a^*_{H^+(aq)}}{a^*_{CO_2(aq)} a_{H_2O(l)}}\right) \tag{10}$$

A similar expression can be obtained for all the reactions given in equations 2-8. Equation 10 can be written in a general form as

$$-\frac{\Delta G_j^0}{RT} = \sum_i v_i \ln a_i \tag{11}$$

ΔG_j^0 is the increment in standard state Gibbs energy for the reaction j. a_i is the activity of species i and v_i is the stoichiometric coefficient of species i, negative for the reactants and positive for the products.

3.2. Vapor-Liquid Equilibria

The following vapor-liquid equilibria were considered.

$$H_2O(l) \rightleftharpoons H_2O(g) \tag{12}$$

$$CO_2(aq) \rightleftharpoons CO_2(g) \tag{13}$$

$$DEEA(aq) \rightleftharpoons DEEA(g) \tag{14}$$

$$MAPA(aq) \rightleftharpoons MAPA(g) \tag{15}$$

The equilibrium condition is that the chemical potential of component i in the aqueous phase is identical to the chemical potential of component i in the gas phase at a given temperature and pressure.

$$\mu_{i(aq)} = \mu_{i(g)} \tag{16}$$

The expression used for the VLE calculations based on criterion given in equation 16 is given below as

$$\frac{\mu_{i(aq)}^{*} - \mu_{i}^{0,ig}(T, P_0)}{RT} + \frac{V_{i(aq)}(P - P_0)}{RT} = \ln\left(\frac{y_i \hat{\phi}_i P}{x_i \gamma_i^* P_0}\right) \tag{17}$$

The expression for the calculation of vapor pressure of pure components (only amines in this work, DEEA and MAPA) is given as

$$-\frac{\Delta G^0}{RT} = \ln\left(\frac{\hat{\phi}_i \gamma_i^\infty P}{P_0}\right) \tag{18}$$

The details of these equations used in the VLE calculations can be found in our previous work [4,10].

3.3. Solid-Liquid Equilibria

The solid-liquid equilibrium considered in this work is given by

$$H_2O(s) \rightleftharpoons H_2O(l) \tag{19}$$

The criterion for the SLE is that the chemical potential is identical in the two phases. The solid compound is in its standard state. Therefore, the chemical potential of the solid compound is equal to its standard state chemical potential. Since ice is the only solid phase formed in the experimental freezing point depression data of both unloaded and CO_2 loaded aqueous amine solutions, equation 11 can be reduced to

$$-\frac{\Delta G^0}{RT} = \ln a_w \tag{20}$$

$\Delta G^0 = \mu_w^0 - \mu_{ice}^0$ is the change in standard state chemical potential between the ice and liquid water and a_w is the activity of water.

3.4. Liquid-Liquid Equilibrium

An important characteristic of the aqueous DEEA-MAPA solutions is that they split into two liquid phases when reacted with CO_2. The equilibrium condition is that the chemical potential of component "i" is identical in the two liquid phases, I and II.

$$\mu_i^I = \mu_i^{II} \tag{21}$$

Since the same standard state is used for each independent component in the two phases, the standard state chemical potential on both sides of equation 21 will cancel out and reduces to the following expression

$$a_i^I = a_i^{II} \tag{22}$$

a_i^I and a_i^{II} are the activity of component i in the liquid phases I and II, respectively. When liquid-liquid equilibrium is considered, the components are not individual ions, but neutral species formed by the ions. Therefore, the criterion for the LLE calculations is that the activity of each independent component is the same in both liquid phases.

3.5. Excess Enthalpy

Thermal property data such as excess enthalpy are very useful for determination of the UNIQUAC surface area parameter (q) because the contribution to the excess enthalpy is proportional to the q parameter. The symmetrical excess enthalpy for the water-amine system can be calculated by using the Gibbs-Helmholtz equation.

$$\left(\frac{\partial(G^E/RT)}{\partial T}\right)_{P,x} = -\frac{H^E}{RT^2} = x_w\left(\frac{\partial \ln \gamma_w}{\partial T}\right)_{P,x} + x_{DEEA}\left(\frac{\partial \ln \gamma_{amine}}{\partial T}\right)_{P,x} \tag{23}$$

γ_{amine} is the symmetrical activity coefficient of amine which can be obtained from the unsymmetrical activity coefficient of amine.

3.6. Heat of Absorption of CO_2

The heat involved when CO_2 is absorbed in the aqueous amine solutions can be calculated from the energy balance of the absorption process.

$$\Delta H_{abs} = \frac{n_2 H_2 - n_1 H_1 - n_{CO_2} H_{CO_2}}{n_{CO_2}} \tag{24}$$

The details of heat of absorption calculations can be found in previous work [4,10].

4. Standard State Properties

The standard state properties (Gibbs energy and enthalpy of formation, and heat capacity) of different components and species used in this work were taken from the NIST tables given at 25 °C. The values of chemical potential (Gibbs energy) at temperature of interest can be calculated from its values at 25 °C (298.15 K) by using Gibbs-Helmholtz equation.

$$-\frac{d \ln K}{dT} = \frac{d\left(\Delta G^0 / RT\right)}{dT} = -\frac{\Delta H^0}{RT^2} \tag{25}$$

Temperature derivative of the enthalpy of formation of the process give the heat capacity of the species involved in the process as

$$\Delta C_p^0 = \frac{d \Delta H^0}{dT} \tag{26}$$

ΔC_p^0 is the increment in the standard state heat capacity by the process. Three parameter temperature dependent heat capacity correlation used in the model is given as

$$\Delta C_{p,i}^* = a_i + b_i T + \frac{c_i}{T - T_{\Theta,i}} \tag{27}$$

The details of calculations of standard state properties can be found elsewhere [4,10].

5. Model Parameter Estimation

The estimation of model parameters was performed by least-square minimization of the weighted sum of squared residuals (S) as given in equation 28.

$$S = \sum_{P^{vap} data} \left(\frac{P_{\text{calc}}^{vap} - P_{\text{exp}}^{vap}}{0.0125 P_{\text{exp}}^{vap}} \right)^2 + \sum_{VLE\ data} \left(\frac{P_{\text{calc}} - P_{\text{exp}}}{0.06 \left(P_{\text{exp}} + 0.01 \right)} \right)^2 + \sum_{SLE\ data} \left(\frac{\Delta G^0 + RT \sum_i v_i \ln a_i}{0.0015 RT} \right)^2$$

$$+ \sum_{H^E\ data} \left(\frac{H_{\text{calc}}^E - H_{\text{exp}}^E}{100 Rx} \right)^2 + \sum_{H^{Abs}\ data} \left(\frac{H_{\text{calc}}^{Abs} - H_{\text{exp}}^{Abs}}{500 Rx} \right)^2 + \sum_{LLE\ data} \sum_i \left(\frac{\ln a_i^{II} - \ln a_i^I}{0.5} \right)^2 \tag{28}$$

"calc" and "exp" represent the calculated values (by the model) and experimental data. The factors 0.0125, 0.06, 0.0015, 100, 500, and 0.5 are the weighting factors respectively used for the pure amine vapor pressure, vapor-liquid equilibrium (VLE), solid-liquid equilibrium (SLE), excess enthalpy (H^E), heat of absorption (H^{Abs}), and liquid-liquid equilibrium (LLE) data. These weighting factors were optimized on the basis of experience in modeling the H_2O-DEEA-MAPA-CO_2 and its sub-systems.

The deviations between the model calculated results and the experimental data are given in as absolute average relative deviation (AARD)

$$AARD = \frac{1}{n}\sum_n \left| \frac{\Phi_{calc} - \Phi_{exp}}{\Phi_{exp}} \right| \times 100\% \qquad (29)$$

Φ is the type of data and n is the number of data points. "calc" and "exp" represent the calculated data values (by the model) and experimental data respectively.

The modeling strategy consists of parameter estimation of the two sub-systems (H_2O-DEEA-CO_2 and H_2O-MAPA-CO_2) separately followed by the H_2O-DEEA-MAPA-CO_2 system. The parameter estimation for the two sub-systems were started with the calculation of vapor pressures of pure amines followed by the binary CO_2 unloaded data (unloaded freezing point, excess enthalpy and unloaded VLE data) and then ternary CO_2 loaded data (loaded freezing point and VLE data and the heat of absorption data). Once a reasonable set of parameters were obtained for each of the H_2O-DEEA-CO_2 and H_2O-MAPA-CO_2 sub-systems, binary parameters across different species of DEEA and MAPA in the two sub-systems were estimated by using the ternary unloaded data (unloaded freezing point and VLE data). Then quaternary CO_2 loaded data (VLE and heat of absorption data) were introduced and all the pre-estimated parameters were refitted to the experimental data simultaneously to get a new set of parameters. Finally, the LLE data were introduced and a final set of parameters were estimated which can reproduce all data values and describe all data types with a single set of parameters.

94 model parameters and 6 thermodynamic properties were fitted to approximately 1500 experimental data. The 94 model parameters are 6 volume (r) and 6 surface area (q) parameters (for DEEA (aq), DEEAH$^+$ MAPA (aq), MAPAH$^+$, $^+$HMAPAH$^+$, and MAPACOO$^-$), and 41 u_{ij}^0 and 41 u_{ij}^T binary parameters for calculating the interaction energy parameters $u_{ij} = u_{ij}^0 + u_{ij}^T (T - 298.15)$. The 6 thermodynamic properties are the standard state Gibbs energy of formation and standard state enthalpy of formation for the three species DEEA (l), MAPA (l), MAPACOO$^-$.

6. Results and Discussion

6.1. Vapor Pressure

The vapor pressure results of pure DEEA and MAPA at different temperatures are given in Fig. 1 (left image for DEEA and right image for MAPA). Experimental data of vapor pressure of DEEA [13-16] and MAPA [16-18] reported by several authors in the literature are plotted along with the calculated curves. The model describes the vapor pressure data very well. However, some deviations at high temperatures can be observed in DEEA case. For DEEA, the absolute average relative deviations (AARD) between the model results and experimental data are 6.5 % for Steele et al., 2002 [13], 20.3 % for Kapteina et al., 2005 [14], and 5 % each for Klepáčová et al., 2011 [15] and Hartono et al., 2013 [16]. The AARD for all the vapor pressure data together from all the literature sources is 9.9 % for DEEA. For MAPA, the AARD between the experimental data and the model results are 5.4 % for all the data together and individually 2.1 % for Kim et al., 2008 [17], 15.2 % for Verevkin and Chernyak, 2012 [18], and 0.9 % for Hartono et al., 2013 [16].
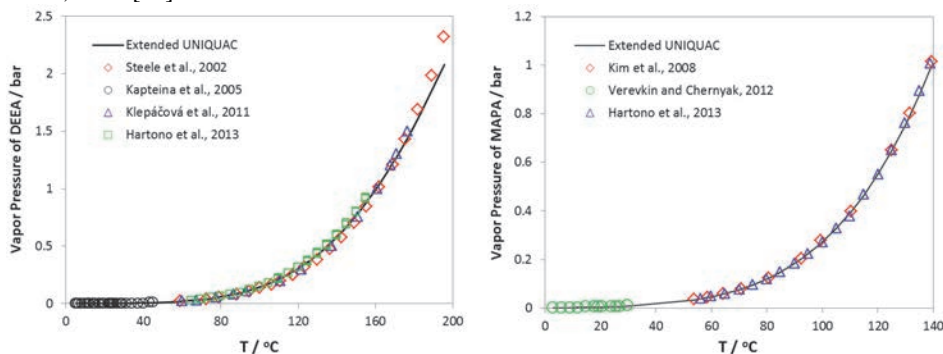

Fig. 1. Vapor pressure of pure amine as a function of temperature: (left) DEEA; (right) MAPA. Experimental data from Steele et al., 2002 [13]; Kapteina et al., 2005 [14]; Klepáčová et al., 2011 [15]; Hartono et al., 2013 [16]; Kim et al., 2008 [17]; Verevkin and Chernyak, 2012 [18].

6.2. Solid-Liquid Equilibrium (Freezing Point Depression)

Freezing point depression data are very important for computing the water activity, a key parameter to estimate the amount of water evaporation in stripping section during solvent regeneration in the capture process [19]. Another important use of freezing point data is to compute the amount of chemical species present in the solution (speciation). Therefore, these data from Arshad et al., 2013 [8] are included in the parameter estimation. Freezing point data in aqueous amines at different concentrations of DEEA, MAPA, and DEEA/MAPA mixtures are plotted with the calculated curves as shown in Fig. 2 (left image for aqueous DEEA and aqueous MAPA solutions and right image for aqueous DEEA/MAPA mixtures). For aqueous DEEA/MAPA mixtures, the freezing point data are plotted as a function of total amine concentration in the solutions for the 5:1, 3:1, 1:1, 1:3, and 1:5 molar ratios of DEEA/MAPA. The model describes the freezing point data very well both in aqueous DEEA and MAPA solutions (left image) and aqueous DEEA/MAPA mixtures (right image) in the whole concentration and temperature range. The estimated AARD for aqueous DEEA is 4.2%, for aqueous MAPA is 3.4 %, and for aqueous DEEA/MAPA blends is 5.2 %.

Similarly, the model calculated freezing points together with the experimental data for CO_2 loaded aqueous DEEA and MAPA solutions are presented in Fig. 3. For CO_2 loaded DEEA system (H_2O-DEEA-CO_2), the freezing point results are presented in left image for four different DEEA solutions (12, 20, 30, and 33 mass %) at a varying CO_2 concentration in the solutions. The right image in Fig. 3 presents the freezing point results for three different aqueous MAPA solutions (10, 20, and 27 mass %) at varying CO_2 concentrations. The model describes the freezing point data very well in both CO_2 loaded systems of aqueous DEEA and MAPA. The AARD between the calculated and the experimental freezing points are 3.5 % for H_2O-DEEA-CO_2 and 3.1 % for H_2O-DEEA-CO_2 systems.
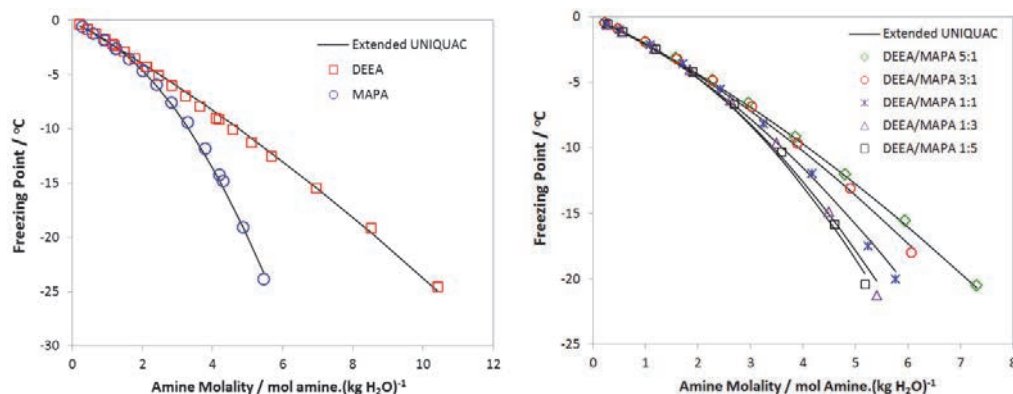

Fig. 2. Freezing point depression as a function of amine molality: (left) aqueous DEEA and MAPA systems; (right) aqueous DEEA-MAPA mixtures. Experimental data from Arshad et al., 2013 [8].
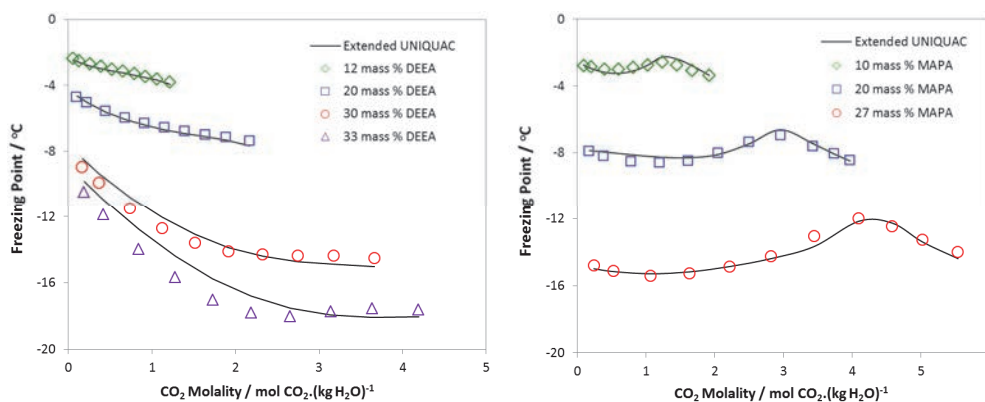

Fig. 3. Freezing point depression as a function of CO_2 concentration: (left) H_2O-DEEA-CO_2 systems at different compositions of DEEA; (right) H_2O-MAPA-CO_2 systems at different compositions of MAPA. Experimental data from Arshad et al., 2013 [8].

6.3. Vapor-Liquid Equilibrium

Vapor-liquid equilibrium data are essential for the design and modeling of unit operations in the capture process [5,20]. The model calculated VLE (both total pressure and CO_2 partial pressure as a function of CO_2 concentration) results of 5M DEEA together with the experimental data from Monteiro et al., 2013 [21] and Arshad et al., 2014 [5] are presented in Fig. 4. A good agreement can be observed between the experimental and the model calculated results both for the total pressure (left image) and CO_2 partial pressure data (right image). However, the model calculated total pressures are slightly higher for the 313.15 K isotherm and slightly lower for the two isotherms at 353.15 K and 393.15 K at high CO_2 concentrations. The estimated AARD between the model results and the experimental data are 7.6 % for Monteiro et al., 2013 [21] and 10.4 % for Arshad et al., 2014 [5] in case of total pressure data, and 19.1 % for Monteiro et al., 2013 [21] in case of CO_2 partial pressure data.

Similarly, Fig. 5 illustrates the model calculated total pressure and CO_2 partial pressure together with experimental data for 2M MAPA system from Arshad et al., 2014 [5] and Pinto et al., 2014 [22]. A fairly good agreement can be seen between that the model results and the experimental data with a few deviations in both the total pressure and CO_2 partial pressure cases. The estimated ARRD between the experimental and the model calculated results is 16.1 % for the total pressure data and 37.2% in case of CO_2 partial pressure data.

The experimental VLE data from Arshad et al., 2014 [5] and the model calculated results for 5M DEEA + 2M MAPA system are presented in Fig. 6 (left image for total pressure and right image for CO_2 partial pressure as a function of CO_2 concentration at different temperatures). The model represents the VLE data very well with some deviations in the results at 353.15 K and 393.15 K for both the cases of total pressure and CO_2 partial pressure.
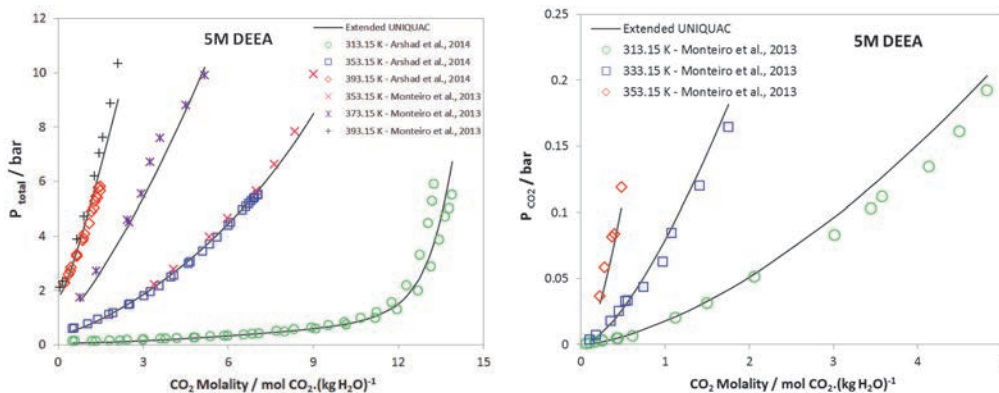

Fig. 4. (left) Equilibrium total pressure and (right) Partial pressure of CO_2 in 5M DEEA solutions as a function of CO_2 composition at different temperatures. Experimental data from Arshad et al., 2014 [5] and Monteiro et al., 2013 [21].
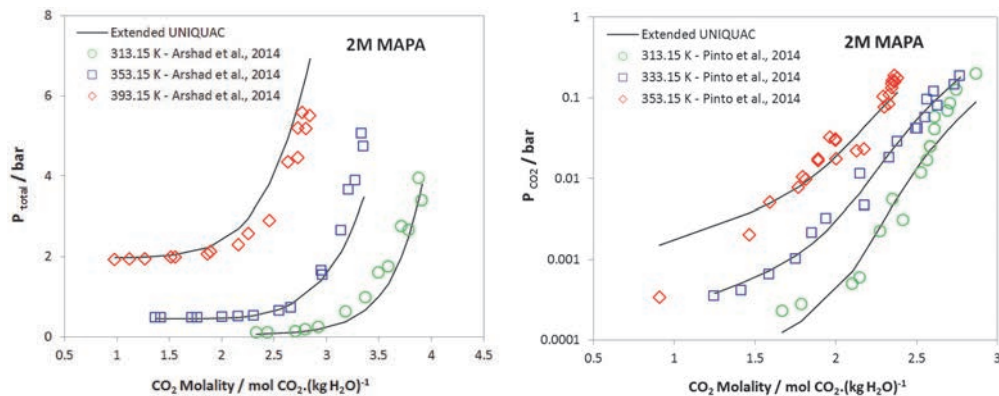

Fig. 5. (left) Equilibrium total pressure and (right) Partial pressure of CO_2 in 2M MAPA solutions as a function of CO_2 composition at different temperatures. Experimental data from Arshad et al., 2014 [5] and Pinto et al., 2014 [22].
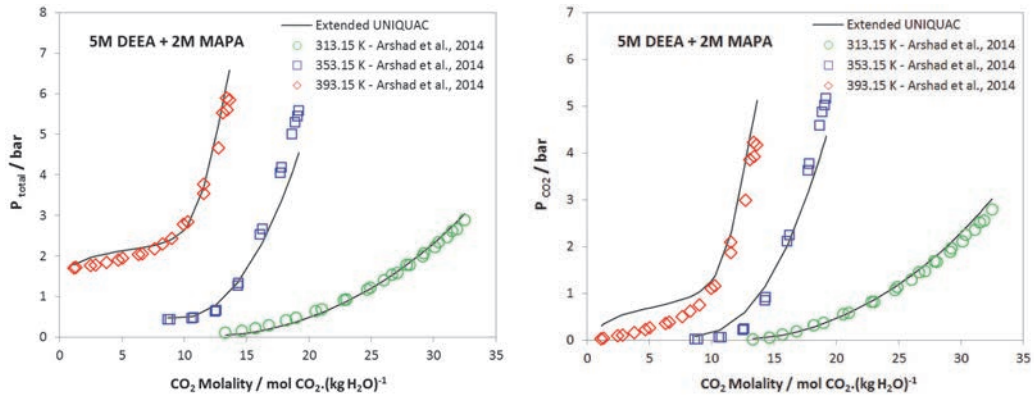
Fig. 6. (left) Equilibrium total pressure and (right) Partial pressure of CO_2 in 5M DEEA + 2M MAPA solutions as a function of CO_2 composition at different temperatures. Experimental data from Arshad et al., 2014 [5].

6.4. Heat of Absorption of CO_2

Heat of absorption of CO_2 in aqueous amines is an important set of data for the thermal performance of the model. Arshad et al., 2013 [6] reported the differential heat of absorption of CO_2 in aqueous DEEA, MAPA, and DEEA/MAPA solutions at different temperatures and these data were included in the parameter estimation. The modeling results together with the experimental data for 5M DEEA, 2M MAPA, and 5M DEEA + 2M MAPA at different temperatures are shown in Fig. 7 (left images for 5M DEEA, center images for 2M MAPA, and right images for 5M DEEA + 2M MAPA). The model represents the differential heat of absorption data very well at all temperatures for all the systems. The estimated deviations (AARD) between the experimental data and the model calculated results are 11.6 % for 5M DEEA, 8.3 % for 2M MAPA, and 6.3 % for 5M DEEA + 2M MAPA.

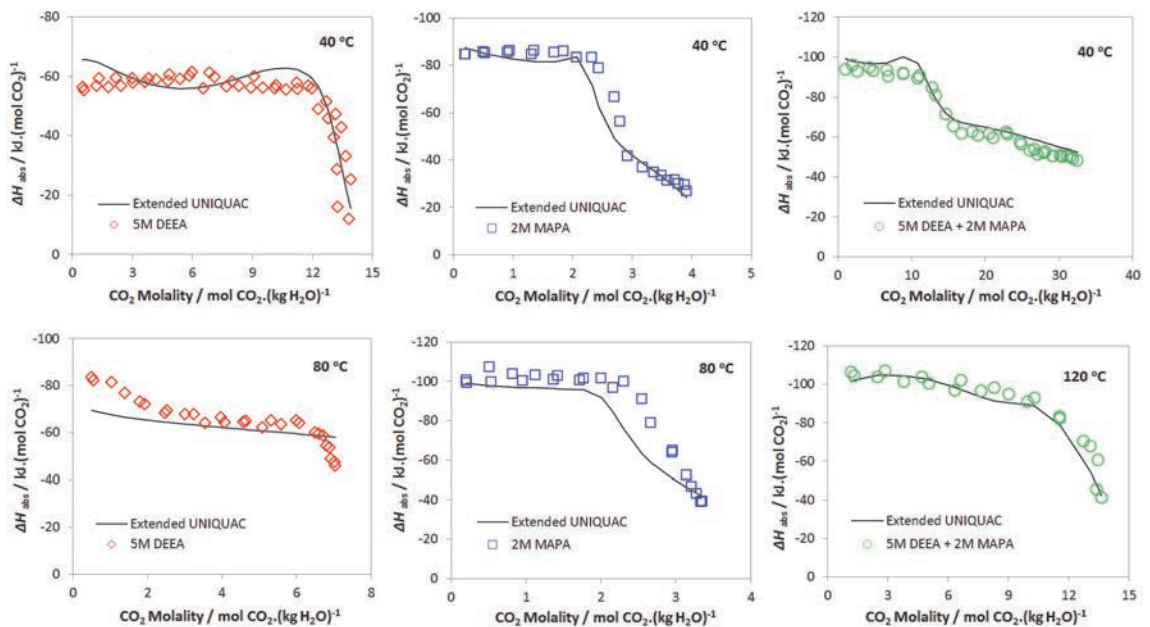Fig. 7. Differential heat of absorption of CO_2 in aqueous amine solutions as a function of CO_2 concentration at different temperatures: (left) 5M DEEA; (center) 2M MAPA; (right) 5M DEEA + 2M MAPA. Experimental data from Arshad et al., 2013 [6].

6.5. Liquid-Liquid Equilibrium

5M DEEA + 2M MAPA blend gives liquid-liquid split upon CO_2 absorption which is one of the main features of this system. It is essential that the model can predict the LLE in the mixed aqueous DEEA-MAPA system. Only 32 LLE data points were available for the parameter estimation from Pinto et al., 2014 [23] at different temperatures. Fig. 8 illustrates the LLE results in H_2O-DEEA-MAPA-CO_2 solutions at 40 °C and 80 °C. The calculated results (binodal curves and tie lines) are plotted in comparison with the experimental data. Left image in Fig. 8 shows the calculated values at 40 °C for the 6 molal MAPA solutions with a constant CO_2 concentration of 4.6 molal and varying DEEA concentrations. To keep the calculations simple and better visualization of the graphs, the model calculations were based on slightly different concentration conditions compared to the experimental data i.e., the MAPA and CO_2 concentrations were not constant in the experimental data but an almost averaged value was used for the model calculations. This simplification allowed the model to calculate the smooth binodal curves and the uniform tie lines which, otherwise, was not possible. Similarly, right image in Fig. 8 represents the model results at 80 °C for the 7.5 molal MAPA solutions with a constant CO_2 concentration of 3.75 molal and varying DEEA concentrations together with the experimental data scattering around the binodal curves.
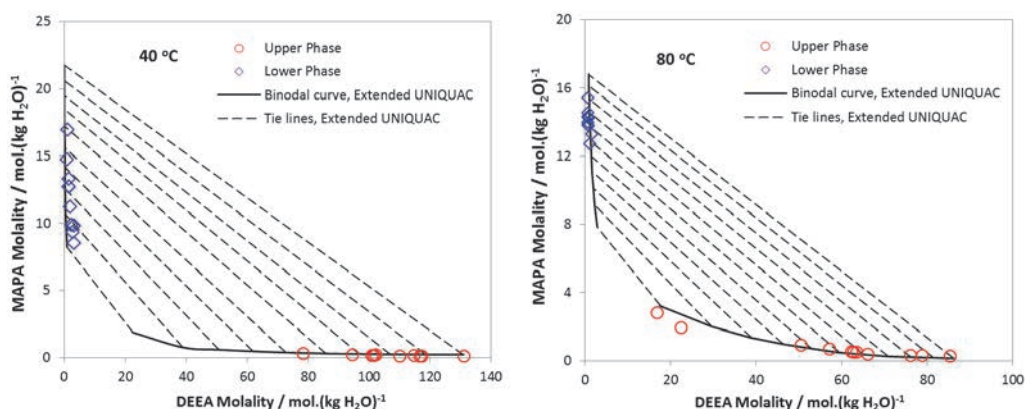

Fig. 8. Modeling results of liquid-liquid equilibrium in H_2O-DEEA-MAPA-CO_2 solutions at different temperatures: (left) Calculated values are for 6 molal MAPA solutions with a constant CO_2 concentration of 4.6 molal and varying DEEA molality at 40 °C; (right) Calculated values are for 7.5 molal MAPA solutions with a constant CO_2 concentration of 3.75 molal and varying DEEA molality at 80 °C. Experimental data from Pinto et al., 2014 [23].

7. Conclusions

The Extended UNIQUAC framework has been implemented in this work to describe the thermodynamics of liquid-liquid phase change DEEA-MAPA solvent system for CO_2 capture. The two sub-systems, H_2O-DEEA-CO_2 and H_2O-MAPA-CO_2, were modeled first followed by the H_2O-DEEA-MAPA-CO_2 system which gives liquid-liquid phase split. Different types of experimental equilibrium and thermal data (pure amine vapor pressure, vapor-liquid equilibrium, solid-liquid equilibrium, liquid-liquid equilibrium, excess enthalpy, and heat of absorption of CO_2 in aqueous amine solutions) were used for the parameter estimation. Ninety four model parameters and six thermodynamic properties were fitted to approximately 1500 experimental data. The model can accurately represent the equilibrium and thermal data for the studied systems with a single unique set of parameters. The model developed in this work can be used for process simulation of CO_2 capture with aqueous blends of DEEA/MAPA.

Acknowledgements

References

[1] Metz, B., Davidson, O., de Coninck, H., Loos, M., Meyer, L. Eds. IPCC Special Report on Carbon Dioxide Capture and Storage. Prepared by Working Group III of the Intergovernmental Panel on Climate Change (IPCC)**,** Cambridge University Press, U.K., 2005.

[2] Tontiwachwuthikul, P., Idem, R. Recent Progress and New Developments in Post-Combustion Carbon-Capture Technology with Reactive Solvents. Future Science Book Series, Future Science Ltd. 2013. DOI: 10.4155/9781909453340.

[3] Liang, Z., Rongwong, W., Liu, H., Fu, K., Gao, H., Cao, F., Zhang, R., Sema, T., Henni, A., Sumon, K., Nath, D., Gelowitz, D., Srisang, W., Saiwan, C., Benamor, A., Al-Marri, M., Shi, H., Supap, T., Chan, C., Zhou, Q., Abu-Zahra, M., Wilson, M., Olson, W., Idem, R., Tontiwachwuthikul, P., 2015. Recent progress and new developments in post-combustion carbon-capture technology with amine based solvents. *Int. J. Greenh. Gas Control* 40, 26-54.

[4] Arshad, M.W., von Solms, N., Thomsen, K., 2016. Thermodynamic Modeling of Liquid-Liquid Phase Change Solvents for CO_2 Capture. *Int. J. Greenh. Gas Control* 53, 401-424.

[5] Arshad, M.W., Svendsen, H.F., Fosbøl, P.L., von Solms, N., Thomsen, K., 2014. Equilibrium Total Pressure and CO_2 Solubility in Binary and Ternary Aqueous Solutions of 2-(Diethylamino)ethanol (DEEA) and 3-(Methylamino)propylamine (MAPA). *J. Chem. Eng. Data* 59 (3), 764-774.

[6] Arshad, M.W., Fosbøl, P.L., von Solms, N., Svendsen, H.F., Thomsen, K., 2013. Heat of Absorption of CO_2 in Phase Change Solvents: 2-(diethylamino)ethanol and 3-(methylamino)propylamine. *J. Chem. Eng. Data* 58 (7), 1974-1988.

[7] Arshad, M.W., von Solms, N., Svendsen, H.F., Thomsen, K., 2013. Heat of Absorption of CO_2 in Aqueous Solutions of DEEA, MAPA and their Mixture, *Energy Procedia* 37, 1532-1542.

[8] Arshad, M.W., Fosbøl, P.L., von Solms, N., Thomsen, K., 2013. Freezing point depressions of phase change CO_2 solvents. *J. Chem. Eng. Data* 58 (7), 1918-1926.

[9] Arshad, M.W., Fosbøl, P.L., von Solms, N., Svendsen, H.F., Thomsen, K., 2014. Equilibrium Solubility of CO_2 in Alkanolamines, *Energy Procedia* 51, 217-223.

[10] Arshad, M.W., 2014. Measuring and Thermodynamic Modeling of De-Mixing CO_2 Capture Systems. Ph.D. Thesis, Technical University of Denmark, Kongens Lyngby, Denmark.

[11] Thomsen, K., Rasmussen, P., Gani, R., 1996. Correlation and prediction of thermal properties and phase behaviour for a class of aqueous electrolyte systems. *Chem. Eng. Sci.* 51, 3675-3683.

[12] Thomsen, K., Rasmussen, P., 1999. Modeling of vapor-liquid-solid equilibrium in gas-aqueous electrolyte systems. *Chem. Eng. Sci.* 54, 1787-1802.

[13] Steele, W.V., Chirico, R.D., Knipmeyer, S.E., Nguyen, A., 2002. Measurements of vapor pressure, heat capacity, and density along the saturation line for cyclopropane acid, *N,N*-diethylethanoalamine, 2,3-dihydrofuran, 5-hexen-2-one, perfluorobutanoic acid, and 2-phenylpropionaldehyde. *J. Chem. Eng. Data* 47, 715-724.

[14] Kapteina, S., Slowik, K., Verevkin, S.P., Heinstz, A., 2005. Vapor pressures and vaporization of a series of ethnaolamines. *J. Chem. Eng. Data* 50, 398-402.

[15] Klepáčová, K., Huttenhuis, P.J.G., Derks, P.W.J., Versteeg, G.F., 2011. Vapor pressures of several commercially used alkanolamines. *J. Chem. Eng. Data* 56, 2242-2248.

[16] Hartono, A., Saleem, F., Arshad, M.W., Usman, M., Svendsen, H. F., 2013. Binary and ternary VLE of the 2-(diethylamino)-ethanol (DEEA)/ 3-(methylamino)-propylamine (MAPA)/ water system. *Chem. Eng. Sci.* 101, 401-411.

[17] Kim, I., Svendsen, H.F., Børresen, E., 2008. Ebulliometric determination of vapor-liquid equilibria for pure water, monoethanolamine, *N*-methyldiethanolamine, 3-(methylamino)-propylamine, and their binary and ternary solutions. *J. Chem. Eng. Data* 53 (11), 2521–2531.

[18] Verevkin, S.P., Chernyak, Y., 2012. Vapor pressure and enthalpy of vaporization of aliphatic propanediamines. *J. Chem. Thermodyn.* 47, 328-334.

[19] Fosbøl, P.L., Randi, N., Arshad, M.W., Tecle, Z., Thomsen, K., 2011. Aqueous Solubility of Piperazine and 2-Amino-2-methyl-1-propanol plus Their Mixtures Using an Improved Freezing-Point Depression Method. *J. Chem. Eng. Data* 56, 5088-5093.

[20] Gaspar, J., Arshad, M.W., Blaker, E.A., Langseth, B., Hansen, T., Thomsen, K., von Solms, N., Fosbøl, P.L., 2014. A Low Energy Aqueous Ammonia CO_2 Capture Process, *Energy Procedia* 63, 614-623.

[21] Monteiro, J.G.M.-S., Pinto,D.D.D., Zaidy, S.A.H., Hartono, A., Svendsen, H.F., 2013. VLE data and modelling of aqueous *N,N*-diethyethanolamine (DEEA) solutions. *Int. J. Greenh. Gas Control* 19, 432-440.

[22] Pinto, D.D.D., Bruder P., Monteiro J.G.M-S., Jens C., Foss C., Hartono A., Svendsen H.F., 2014. Unpublished VLE data and modelling of aqueous *N*-methyl-1,3-diaminopropane (MAPA) solutions.

[23] Pinto, D.D.D., Zaidy, S.A.H., Hartono A., Svendsen H.F., 2014. Evaluation of a phase change solvent for CO_2 capture: Absorption and desorption tests. *Int. J. Greenh. Gas Control* 28, 318-327.